International Conference on Mathematics and Computational Methods Applied to Nuclear Science and Engineering (M&C 2011)
Rio de Janeiro, RJ, Brazil, May 8-12, 2011, on CD-ROM, Latin American Section (LAS) / American Nuclear Society (ANS)
ISBN 978-85-63688-00-2

MONTE CARLO SIMULATION OF A CODED-APERTURE THERMAL NEUTRON CAMERA

I. Dioszegi and C. Salwen
Nonproliferation and National Security Department
Brookhaven National Laboratory
Upton, New York 11973-5000 USA.
dioszegi@bnl.gov; salwen@bnl.gov

L. Forman
Ion Focus technology, Inc.
52 Pardam Knoll Road
Miller Place, New York 11764 USA
lforman@bnl.gov

ABSTRACT

We employed the MCNPX Monte Carlo code to simulate image formation in a coded-aperture thermal-neutron camera. The camera, developed at Brookhaven National Laboratory (BNL), consists of a 20x17 cm^2 active area ^{3}He-filled position-sensitive wire chamber in a cadmium enclosure box. The front of the box is a coded-aperture cadmium mask (at present with three different resolutions). We tested the detector experimentally with various arrangements of moderated point-neutron sources. The purpose of using the Monte Carlo modeling was to develop an easily modifiable model of the device to predict the detector's behavior using different mask patterns, and also to generate images of extended-area sources or large numbers (up to ten) of them, that is important for nonproliferation and arms-control verification, but difficult to achieve experimentally. In the model, we utilized the advanced geometry capabilities of the MCNPX code to simulate the coded aperture mask. Furthermore, the code simulated the production of thermal neutrons from fission sources surrounded by a thermalizer. With this code we also determined the thermal-neutron shadow cast by the cadmium mask; the calculations encompassed fast- and epithermal-neutrons penetrating into the detector through the mask. Since the process of signal production in ^{3}He-filled position-sensitive wire chambers is well known, we omitted this part from our modeling. Simplified efficiency values were used for the three (thermal, epithermal, and fast) neutron-energy regions. Electronic noise and the room's background were included as a uniform irradiation component. We processed the experimental- and simulated-images using identical LabVIEW virtual instruments.

Key Words: Monte Carlo calculations, neutrons, coded aperture imaging.

1. INTRODUCTION

More than 50 years ago, the concept was introduced of imaging non-focusable radiation via coded apertures [1]. Whilst pinhole cameras can produce images with non-focusable radiation, the loss in intensity due to the small aperture prohibits practical applications except for representing very bright sources. Coded aperture devices essentially are pinhole cameras with a

large number of pinholes arranged specifically, such that the original image can be reconstructed using decoding algorithms. Fenimore et al. patented a specific case, using uniformly redundant arrays, in 1980 [2].

Coded-aperture devices have seen many applications, mainly in the field of astrophysics. However, the principles of coded-aperture imaging are applicable to other radiations, where it is possible to realize the pinhole patterns, and create transparent and radiation-blocking pixels. Thermal neutrons have an extremely high capture cross-section in cadmium, so allowing us to build a coded-aperture neutron camera using cadmium to create the opaque pixels.

In the late nineties, Brookhaven National Laboratory (BNL) developed a coded-aperture thermal-neutron-imaging device [3]. It consists of a 20x17 cm^2 active area ^{3}He-filled position-sensitive wire chamber in a cadmium enclosure box. The front of the box is a coded aperture mask (at present with three different resolutions). This device demonstrably can image distant thermal-neutron sources (up to 64 m), and arrangements of multiple sources from a shorter distance (up to 4 m). This capability for searching for distant or shielded sources makes the device useful for applications in homeland security and nonproliferation; imaging multiple sources is important for treaty verifications.

We present here the first results of our work to simulate this thermal-neutron camera using the Monte Carlo code MCNPX [4]. These simulations serve multiple purposes. They help to develop and debug the image-reconstruction software by providing data wherein the source (and the energy and directional distribution of neutrons) is predetermined and exactly known, and are able to create and evaluate scenarios that are difficult to realize experimentally, such as sources shielded by different configurations, or multiple source arrangements.

There are components of the problem that can be simulated without a great deal of simplification: Among them are the source (the geometry and the energy distribution of the source neutrons), the cadmium mask, and the propagation of the neutrons from the source to the active area of the detector. However, the MCNPX cannot follow the process of signal production in the detector itself. This involves the movement of electrons and ions in the gas to the wires/strips, and then charge-division and amplification, all of which generate the x-y coordinates of the individual neutron hits. In this part of the simulation, we will use some simplifications. Cadmium is known to absorb all thermal neutrons up to its threshold (~0.3 eV). In this energy region, the mask is considered a perfect one. For epithermal neutrons, the cadmium mask is semi-transparent, and only attenuates the neutrons. The efficiency of epithermal neutrons still is significant enough to create a signal in the detector gas. Fast neutrons penetrate the mask with minimal or no attenuation. The efficiency of a pure ^{3}He gas detector is small for fast neutrons. We have ~20% propane mixed into the ^{3}He in our detector, and hence, it has some efficiency for fast neutrons as well, where the mask is inefficient. To adjust the detector's efficiency as a function of energy we will use scaling numbers, and verify them by comparisons to experimental data.

2. MONTE CARLO CALCULATIONS

In the following, we describe the Monte Carlo calculations undertaken for different parts of the detection process, starting from the neutrons created by the fissioning neutron source, continuing with our simulation of the coded aperture mask, and then analyzing the neutrons penetrating the detector and creating the images.

2.1. Simulation of the Neutron Source and the Moderated Neutron Spectrum

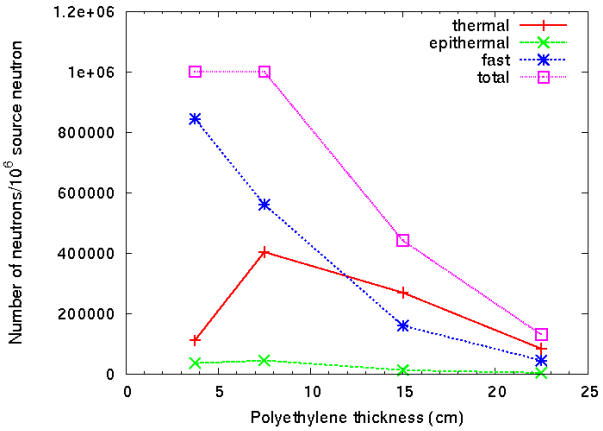

Figure 1. Thermalization of ^{252}Cf fission neutrons in polyethylene. In the MCNPX calculation, we used 10^6 fission neutrons thermalized by polyethylene spheres with different radii (the source was centered). The lines connecting the calculated data points are only to guide the eye.

In our simpler experiments, we imaged a point-like ^{252}Cf source surrounded by a few-cm-thick polyethylene thermalizer. As a first step, we simulated this simple setup by a point source inserted in the middle of a polyethylene sphere (radius of 3.75 cm). We tallied the neutron flux on the surface of the sphere as a function of energy, using three energy bins, one for thermal neutrons, one for epithermal neutrons, and one for the fast ones. Figure 1 gives an example of the calculated ratios for each kind. The thermal-neutron flux reaches maximum at ~7.5 cm thickness of polyethylene. At larger thickness, the polyethylene starts to absorb the neutrons. Similar calculations can be undertaken with the Monte Carlo code for more complex source geometries, and for multiple sources.

2.2. Simulation of the Coded Aperture Mask and Testing with Mono-energetic Thermal Neutrons

2.2.1. The modified uniformly redundant array (MURA) mask

The most important task in simulating a coded-aperture detector is to assess the shadow of the mask cast by a point source on the detector's active area. The advanced geometrical capability of MCNPX supports this task in a relatively simple manner, In our simulation, the mask was

represented via the code's "repeated structures" feature. First, we calculated a 19x19 array representing the modified uniformly redundant array (MURA) using an independently written LabVIEW routine. This array (consisting of zeros and ones, respectively, for the holes and the blocked cells in the array) then was used in the "repeated structure" part of the input file, wherein we replaced the zeros and ones by different numbers pointing to different materials (air for the holes, and cadmium for the blocked parts). To increase the detector's view angle, we employ a four-fold mask, tiled from identical masks. Figure 2 shows the resulting image of the four-fold mask itself, plotted using MCNPX.

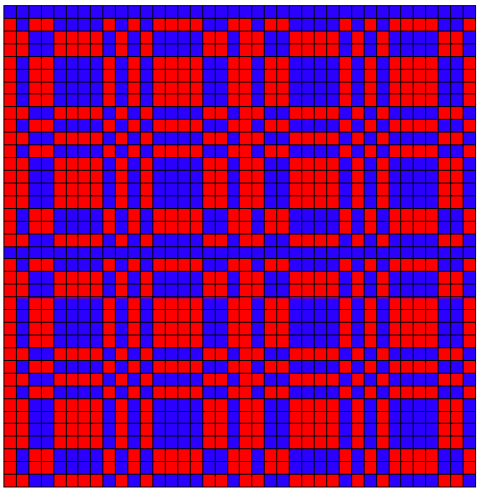

Figure 2. MCNPX model of the four-fold 19x19 pixel-coded aperture mask. Red cells are open pixels, and the blue cells are cadmium pixels.

After creating the input geometry of the mask, we used this section of the input to create the initial model. We represented the wire grid by a mesh tally, in which the mesh had the same dimensions as the detector's active area (20x17 cm^2), with a pixel size corresponding to the array size of the data acquisition board (608x512) that over-samples the detector's resolution by a factor of ~3. We tallied the neutron flux using these mesh tallies.

For initially testing the model, we used a point source of thermal neutrons, and temporarily we made the cadmium cells in the mask nontransparent for neutrons (by setting the cell importance to 0). To speed up the calculations, we restricted the neutrons coming from the source to a cone, by this method eliminating the wastage of computational time for particles that do not hit the mask or the detector (this condition could be relaxed later to include scattering in the air).

The resulting mesh tally first was converted to binary file, and then processed by the LabVIEW routine, which originally was written to process experimental data with the coded-aperture detector. This routine is detailed elsewhere [5]. It involves constructing a matrix G in which the mask's open pixels correspond to +1 , and the closed ones to -1. The reconstruction itself is accomplished by generating digital fast Fourier-transforms of the data array and mask pattern. A scalar multiplication of the matrix elements and the inverse Fourier transform of the product generate the final image. Figure 3 is the resulting image from our first simulated data, where the source was emitting only thermal neutrons.

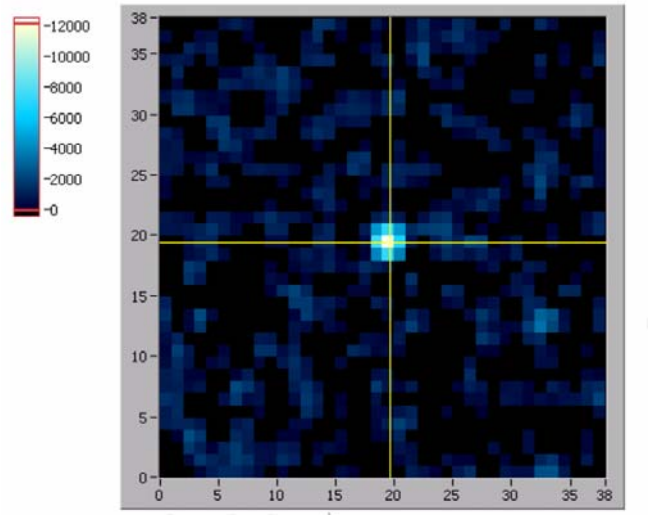

Figure 3. Simulated image of a point source in 2m distance, centered, emitting thermal neutrons and using a "perfect" mask that is 100% opaque for the filled pixels. The image shows an extremely high peak-to-background ratio.

Statistical analysis of this image revealed an unrealistically high peak-to-background ratio, obtained by comparing the brightest pixel in the image to the fluctuations, the latter being estimated by the square root of the total counts in the detector. This occurred because we used a perfect mask, which is 100% transparent in open pixels, and blocks 100% of the thermal neutrons in the closed pixels. Therefore, in the next phase of the simulation we included in the mask semi-transparency to epithermal neutrons, the almost full transparency to fast neutrons, with the known efficiencies of the detector for these three neutron energies.

2.3. Simulations with More Realistic Neutron-Energy Distributions

2.3.1. Experimental results for a single thermalized ^{252}Cf source

To assure collecting good quality experimental data with our thermal-neutron camera, where all the relevant parameters are well known, we recorded a 3600 s image of a thermalized, relatively strong (~10^5 neutron/sec) ^{252}Cf source centered in a 3x3 inch polyethylene cube. The source was on the central axis of the detector, and the distance from the detector's mask was 200 cm. Figure 4 shows the reconstructed image. The left panel depicts the raw image recorded by the detector, the rectangular area (marked by the four cursors) we used for the reconstruction, while the right panel displays the final image. We determined the size of the rectangular area by simple geometrical calculation. It depends on the distance of the source from the mask, the distance from the mask to active area (the camera's "focal length"), and the dimensions of the mask itself.

The reconstructed source image is slightly off-center, which we believe due to inaccuracy in positioning the source setup. The image reconstruction program calculates the ratio of the brightest pixel to the background fluctuation, which is ~70 in this picture.

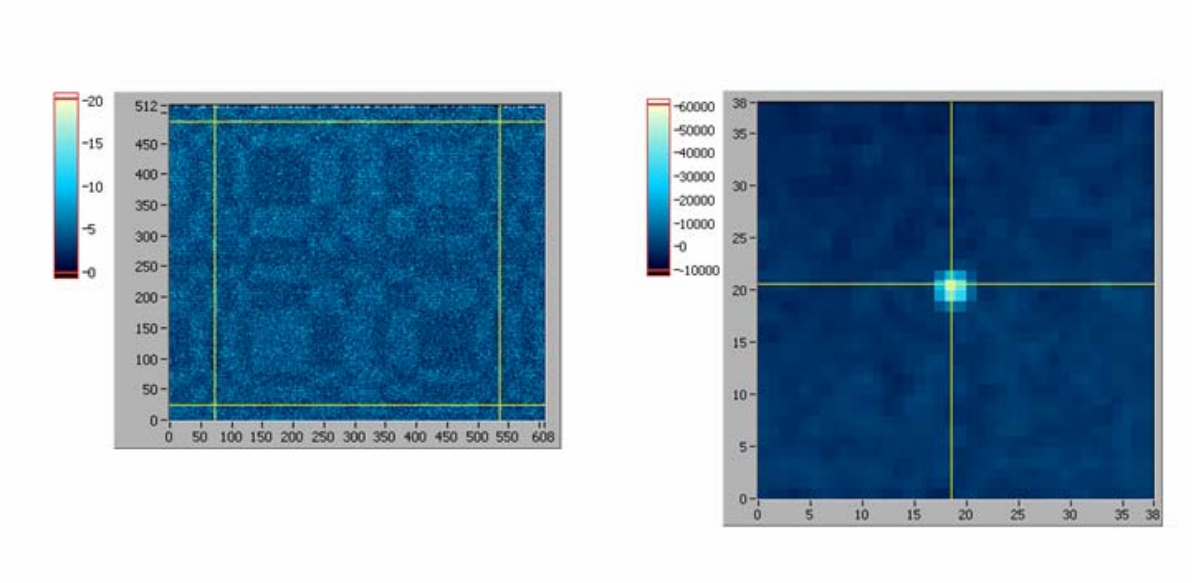

Figure 4. Left panel: Recorded shadow image of one thermalized source from 2 m distance, as seen by the detector. For one source, the mask's pattern is clearly visible. The image reconstruction routine used the selected area (shown by the yellow cursors) to generate the image on the right.

2.3.2. (Semi) transparency of the cadmium mask for epithermal- and fast-neutrons

A reliable simulation requires accounting for the efficiency of the cadmium mask for neutrons of different energies. The cadmium mask has a huge absorption cross-section (~10^5 barn for thermal neutrons) up to the cadmium threshold energy of ~0.3 eV. For epithermal neutrons ranging from 0.3 eV-2 eV it is semi-transparent, and becomes fully transparent for higher energy (fast) neutrons. The transparency of the mask for epithermal- and fast-neutrons increases the scattered background in the images.

In our more advanced simulations, we approximated this transparency effect in the following way. The emission of the fast-neutron source in polyethylene thermalizer is determined in the first simulation run in three energy bins, which tally the flux of the thermal-, epithermal-, and fast-neutrons. In the following run, we setup in MCNPX an extended area neutron source (the shape of which approximated the source's thermalizer material), and defined the source's emission strength in three bins (thermal, epithermal, and fast) with the source's intensity ratios determined by the previous full-source calculation. We applied another computational trick: We restricted the emission from the source to a cone directing the neutrons towards our detector. Although it always is possible to start with the fast-neutron source and the thermalizer, the approximation steps outlined above greatly reduce computing time. This is especially important when running simulations with an identical source setup, but changing other parameters, such as the detector's distance, mask's location. However, our approximation neglects the neutron-scattering effect in the air, and the surrounding area, e.g., room's floor, and walls.

Having approximated the source emission in three energy bins, we then generate the final image as superposition of three images. There are two possible ways to do this: 1) Superimpose the

raw images (detector counts) and run the image-reconstruction code once, or 2) create three reconstructed images from the three components (thermal-, epithermal- and fast-neutrons), and superimpose the three reconstructed images to a final picture. We elected the second method because we found it more intuitive.

The first component is the image of thermal neutrons. Here, the mask is opaque, and the detector efficiency is ~80% [6]. The second component is obtained from the transmitted epithermal flux (calculated by MCNPX). The detector efficiency for epithermal neutrons is about 20% [6]. The third component is calculated from the transmitted flux of fast neutrons that essentially gives a uniform background irradiation, where the mask has no effect. We are not aware of any published data on the detector's efficiency in this region. Therefore, we used a small ^{252}Cf source of known intensity to determine it; our measured value was <1%.

The final step in the calculation is to mix the three components with their corresponding efficiencies as weighting factors. Illustrated in Figure 4 is the result of our simulating one ^{252}Cf source placed in a 1.75 cm thick polyethylene thermalizer and at a distance of 200 cm from the center of the detector mask.

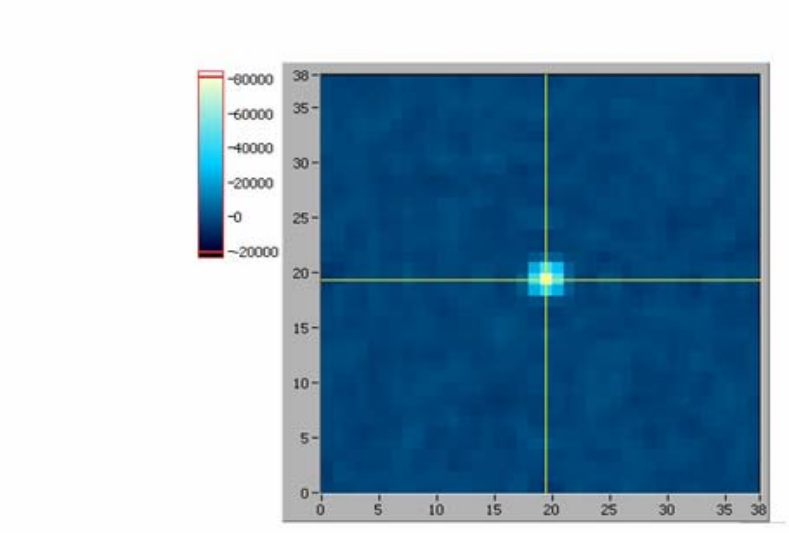

Figure 5. Result of the simulation wherein the thermal-, epithermal-, and fast- neutron images are mixed according to their efficiency weighting ratios.

The original reconstruction gives a very high peak-to-background ratio. To match the measured value (~70) above, besides matching the number of simulated particles hitting the face of the detector, we had to increase the ratio of the fast neutron component to ~25%. This increase helps to describe the events originating from scatter in the room (those neutrons do not come directly from the point source), and from the electronic- and other noise in the detector, which also have a uniform contribution.

With the procedure outlined above we were able to simulate the thermalized point-source, not only accurately describing its position, but also finding a similar peak-to-background noise ratio, as determined experimentally. During image processing, we used the same routines for the

experimental- and simulated-data, modified only to include the mixing of the three different images generated by the thermal-, epithermal-, and fast-neutrons.

3. CONCLUSIONS

We undertook MCNPX simulations of our coded-aperture thermal-neutron camera. The main steps of the work included simulating the MURA mask, and the thermalized neutron source (creating a simplified source based on the results), and generating images of the thermal-, epithermal-, and fast-neutrons. The final simulated image is a superposition of the three images with their weighting factors, reflecting the efficiency of the detector in the different energy regimes. The room's background was added by further increasing the fast-neutron component.

We used MCNPX to generate data that we processed with our existing LabVIEW image-reconstruction routines. We calibrated our calculations to the experimental data obtained for a thermalized point-source.

Our newly developed simulation tool is capable of modeling scenarios that are difficult to achieve experimentally (complicated shielding, or multiple sources). It also will be very efficient in examining the effects of different detector geometries and mask patterns.

ACKNOWLEDGMENTS

We are indebted to Dr. P. E. Vanier, who (in collaboration with L. Forman) originally developed the coded aperture neutron detector, and who wrote the original image processing software.

REFERENCES

1. L. Mertz and N. Young, Proc. *Conf. Optical Instruments and Techniques*, London 1961, p. 305.
2. E. E. Fenimore and T. M. Cannon, Coded aperture imaging with uniformly redundant arrays. United States Patent 4360797 1980.
3. P. E. Vanier and L. Forman, Forming Images with Thermal Neutrons. SPIE International Symposium on Optical Science and Technology, Conference 4784A, Hard X rays, Gamma Rays and Particles, Seattle, WA, July, 2002.
4. D. Pelowitz (Ed.), MCNPX User's Manual Version 2.6.0, *Los Alamos National Laboratory report LA-CP-07-1473* (April 2008).
5. P. E. Vanier, Improvements in coded aperture thermal neutron imaging. Penetrating Radiation Systems and Applications V, edited by F. Patrick Doty, H. Bradford Barber, Hans Roehrig, Proc. of SPIE Vol. 5199 (SPIE, Bellingham, WA, 2003.) p.124.
6. Report No BNL325, Brookhaven National Laboratory. The efficiency as a function of gas pressure was calculated from neutron capture cross section data in: Garber, D.I. & Kimsey, R.R. (1976) Neutron cross sections Volume II curves.